Biol Cybern (2005)
DOI 10.1007/s00422-005-0005-0

LETTER TO THE EDITOR

Biological Cybernetics

**Jan-Moritz P. Franosch · Andreas B. Sichert
Maria D. Suttner · J. Leo van Hemmen**

Estimating position and velocity of a submerged moving object by the clawed frog *Xenopus* and by fish—A cybernetic approach

Received: 1 July 2005 / Accepted: 5 July 2005

Abstract The lateral-line system is a unique facility of aquatic animals to locate predator, prey, or conspecifics. We present a detailed model of how the clawed frog *Xenopus*, or fish, can localize submerged moving objects in *three* dimensions by using their lateral-line system. In so doing we develop two models of a slightly different nature. First, we exploit the characteristic properties of the velocity field, such as zeros and maxima or minima, that a moving object generates at the lateral-line organs and that are directly accessible neuronally, in the context of a simplified geometry. In addition, we show that the associated neuronal model is robust with respect to noise. Though we focus on the superficial neuromasts of *Xenopus* the same arguments apply *mutatis mutandis* to the canal lateral-line system of fish. Second, we present a full-blown three-dimensional reconstruction of the source on the basis of a maximum likelihood argument.

Keywords clawed frog Xenopus · underwater localization of moving objects · neuronal model · superficial neuromasts

1 Introduction

The lateral-line system is a mechanoreceptive system for the detection and analysis of water movements along an animal's body. It is found in fish, tadpoles, and adult aquatic amphibians. These animals use it to detect the velocity or pressure of the surrounding water for catching prey, communicating with conspecifics, or navigation (Russell 1976, Hassan 1985, Coombs and Fay 1993, Bleckmann 1994, Coombs et al. 2000). A typical example, which we will analyze in detail, is the clawed frog, *Xenopus laevis laevis*, which is dominantly aquatic and will be henceforth called *Xenopus*. It is nocturnal and lives mainly in turbid stagnant waters. Its eyes are not adapted to seeing in water and the animal's lateral-line system has become the central sensory system for spatial orientation (Elepfandt 1996). *Xenopus* uses this system for catching prey in water. When an insect drops onto the water surface, a wave is generated that passes along *Xenopus* and the frog will turn toward the wave's origin, its prey. This localization is done by means of the frog's lateral-line system (Kramer 1933).

In *Xenopus* the lateral-line system's detectors comprise approximately 180 small superficial lateral-line organs distributed in various lines along the sides of the body, around the eyes, and at a few other locations of head and neck. See Fig. 1 for *Xenopus* with lateral-line organs; the reader may consult Russell (1976) or Tinsley and Kobel (1996) for a review. Each lateral-line organ contains small cupulae, gelatinous flags protruding into the water, which are deflected as a consequence of the local water velocity (Kalmijn 1988). The cupulae are only sensitive to the water velocity in one direction in that they measure the projection of the velocity vector onto the direction of maximal sensitivity (Görner 1963, Görner and Mohr 1989).

The lateral line of fish responds to submerged moving objects (Engelmann et al. 2003). There are similar results for *Xenopus* (Görner and Mohr 1989, Kramer 1933, Elepfandt 1984). Franosch et al. (2003, 2005) have developed a mathematical model for prey localization at the water *surface*. Here we construct a mathematical model that allows *Xenopus* to localize a *submerged* moving object in *three* dimensions and determine its velocity vector.

2 Hydrodynamics of the stimulus

For simplicity, we assume that the object that is to be detected is a moving sphere; cf. Fig. 2 for the streamlines.

For further analysis, the water velocity is needed at the positions of *Xenopus'* lateral line organs because the deflection $y_i(t)$ of cupula i is roughly proportional to the local velocity (Russell 1976, Kalmijn 1988). In an ideal fluid, a moving sphere with radius a and velocity $\mathbf{w}$ at the origin of

J.-M. P. Franosch · A. B. Sichert · M. D. Suttner · J. L. van Hemmen
Physik Department, TU München,
85747
Garching bei München, Germany,
E-mail: jfranosc@ph.tum.de

Fig. 1 The clawed frog *Xenopus laevis laevis*. Its lateral line organs can be clearly seen as white "stitches"

the coordinate system generates a velocity potential as due to a dipole (Lamb 1932)

$$\phi(\mathbf{r}) = \frac{a^3}{2r^3}\,\mathbf{w}\cdot\mathbf{r}\,.$$

The negative gradient of the velocity potential is the water velocity at position $\mathbf{r}$,

$$\mathbf{v}(\mathbf{r}) = -\nabla\phi(\mathbf{r}) = \frac{a^3}{2r^5}\left[3(\mathbf{w}\cdot\mathbf{r})\,\mathbf{r} - \mathbf{r}^2\,\mathbf{w}\right]\,. \tag{1}$$

If, as shown below, the body of *Xenopus* does not significantly influence this velocity field then *Xenopus* can never detect the size of a moving sphere but only the product $a^3 w$ of the third power of the radius of the sphere and size $w := \|\mathbf{w}\|$ of its velocity. Experiments indeed show that the absolute size of the object cannot be determined independently of its velocity (Vogel and Bleckmann 2001).

We can calculate the water velocity at position $\mathbf{r}$ caused by a moving sphere at $\mathbf{r}_0$ as $\mathbf{v}(\mathbf{r}-\mathbf{r}_0)$. The cupulae of lateral-line organ number i, $1 \le i \le 180$, at position $\mathbf{r}_i$ measure the projection v_i of the water velocity $\mathbf{v}(\mathbf{r}_i - \mathbf{r}_0)$ onto the direction of maximal sensitivity $\mathbf{s}_i$ of the cupulae.

$$v_i = \mathbf{s}_i \cdot \mathbf{v}(\mathbf{r}_i - \mathbf{r}_0), \quad \|\mathbf{s}_i\| = 1 \tag{2}$$

We combine all cupulae of each lateral-line organ because the different cupulae are approximately at the same position $\mathbf{r}$ and point into the same direction $\mathbf{s}_i$. Of course, *Xenopus'* body influences the velocity field in the fluid. However, as shown in Fig. 3, its influence is small.

Equations (1) and (2) show that the lateral-line response v_i of organ i is linearly dependent on the velocity $\mathbf{w}$ of a moving object. By implicitly defining the vector $\mathbf{t}_i$, we can therefore write

$$v_i = \mathbf{t}_i(a, \mathbf{r}_i - \mathbf{r}_0)\cdot\mathbf{w} \tag{3}$$

According to Eqs. (1) and (2), with $\mathbf{p}_i := \mathbf{r}_i - \mathbf{r}_0$, we get for $\mathbf{t}_i$

$$\frac{a^3}{2r^5}\begin{pmatrix} s_{ix}(3p_{ix}^2 - \mathbf{p}_i^2) & +3s_{iy}p_{ix}p_{iy} & +3s_{iz}p_{ix}p_{iz} \\ 3s_{ix}p_{iy}p_{ix} & +s_{iy}(3p_{iy}^2 - \mathbf{p}_i^2) & +3s_{iz}p_{iy}p_{iz} \\ 3s_{ix}p_{iz}p_{ix} & +3s_{iy}p_{iz}p_{iy} & +s_{iz}(3p_{iz}^2 - \mathbf{p}_i^2) \end{pmatrix}$$

We combine all v_i into a 180-dimensional vector $\mathbf{v} := (v_1, \ldots, v_{180})$, define the 180×3-matrix T by its rows $\mathbf{t}_i$, i.e., $T_{ij} = (\mathbf{t}_i)_j$, write

$$\mathbf{v} = T(a, \mathbf{r}_0)\mathbf{w}\,, \tag{4}$$

and get a simple linear expression to be used later on for the measured velocities $\mathbf{v}$ on *Xenopus'* skin, given the velocity $\mathbf{w}$, the position $\mathbf{r}_0$, and the radius a of the moving object.

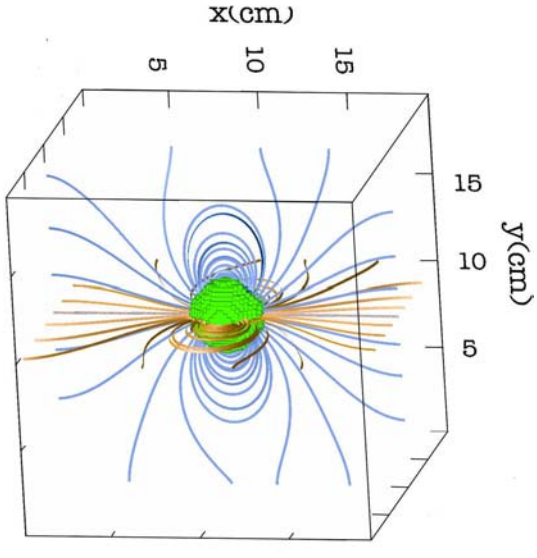

Fig. 2 The streamlines in an incompressible fluid caused by a sphere (green) moving in x-direction. Streamlines in the x-y-plane are depicted blue, streamlines in the x-z-plane in orange. The numerical calculation was performed on a $100 \times 100 \times 100$ grid using the SOR method (Young 1971, Roache 1972, Hackbusch 1986, Marsal 1989, Griebel et al. 1995, Press et al. 1995, Braess 2003, Varga 1999)

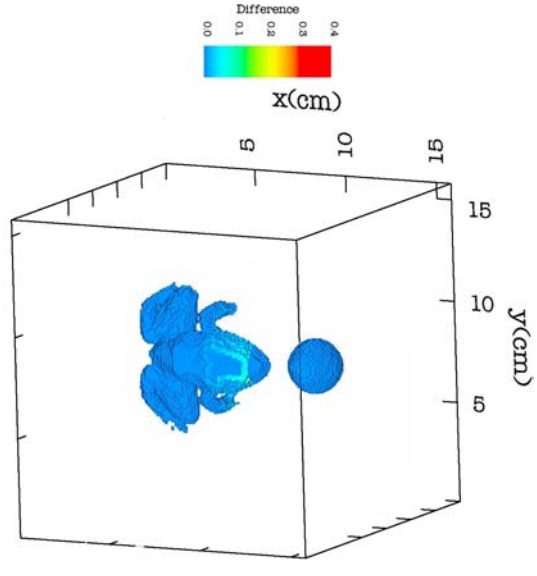

Fig. 3 The relative difference between the approximation (2) and the numerically calculated velocity at *Xenopus'* body is color-coded. As the differences are small (less than about 20 %, corresponding to yellow color), the approximation is appropriate. The calculation has been performed on a $160 \times 160 \times 160$ grid. The sphere moves in x-direction right away from the frog

3 Model A: Short-range detection

We now assume that the prey moves very near to *Xenopus'* skin. In experiments, fish can localize prey that moves less than a fish length away from the fish's body. Moreover, in experiments with the mottled sculpin (Coombs and Conley 1997, Coombs 1999), the fish approaches a source stepwise. First, it turns one side of its body in parallel to the axis of motion of the prey. Second, the fish approaches the source frontally. The fish repeats the two steps until it is near enough for the final strike. In the following, we develop a very simple model for underwater prey detection of *Xenopus* that also accounts for experiments on the mottled sculpin.

3.1 The stimulus and its properties

A prey moves with velocity $\mathbf{w} = (w_x, w_y, w_z)$ and has radius a. For simplicity, we assume it is located in the x, y-plane. Of course, *Xenopus* can only measure the projection of the velocity field onto its skin. From (1) we get

$$v_x(\mathbf{r}) = \frac{a^3}{2}\left[3\frac{(w_x x + w_y y)\,x}{(x^2+y^2)^{\frac{5}{2}}} - \frac{w_x}{(x^2+y^2)^{\frac{3}{2}}}\right]. \qquad (5)$$

at position $\mathbf{r} = (x, y, 0)$. As we only account for short-range detection here, we neglect the curvature of the frog's skin and assume that the lateral-line organs lie in a line parallel to the x-axis, as depicted in Fig. 4; the fish analogy is evident.

Figure 5 shows the water velocities v_x along the line of lateral-line organs for several values of $c := w_y/w_x = \tan\alpha$, where α denotes the angle between the lateral-line array and $\mathbf{w}$.

Say, the prey is at position (x_0, d) and a lateral-line organ is at position $(x, 0)$. Then $\mathbf{r} = (x - x_0, -d)$. In the following we show that *Xenopus* is able to compute both the prey's position and the direction c of its velocity by measuring only characteristic points, such as the zeros and the extrema of $v_x(x)$, since these are *neuronally* easily accessible (Hofmann et al. 2004). The zeros of v_x are at

$$x_\pm = \frac{1}{4}d\left(3c \pm \sqrt{9c^2+8}\right) + x_0\,. \qquad (6)$$

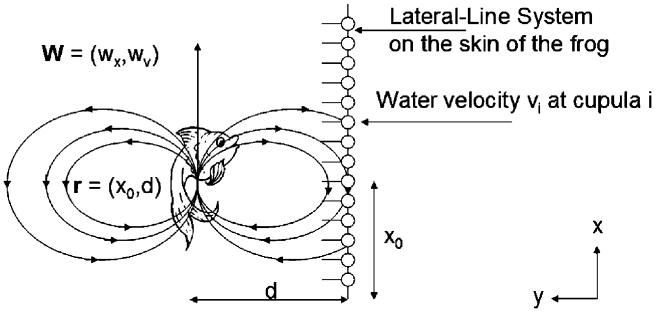

Fig. 4 Lateral-line organs are arranged parallel to the x-axis. A prey at position (x_0, d) is moving with velocity $\mathbf{w} = (w_x, w_y)$ and has momentary distance d

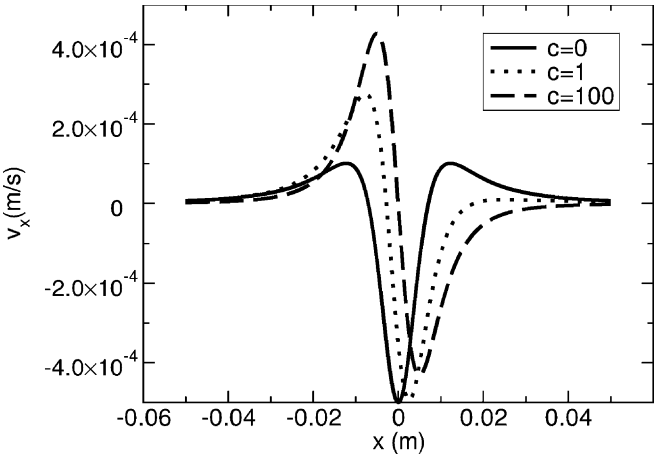

Fig. 5 The water velocity v_x along the line of lateral-line organs for a prey with radius $a = 1$ mm, distance $d = 1$ cm, position $x_0 = 0$ and prey velocity $w = 0.1$ m/s for different values of c. For $c = 0$ the graph is symmetric. The graph becomes antisymmetric for large values of c, when $\mathbf{w}$ is practically orthogonal to the lateral-line system of Fig. 4

With the abbreviations

$$\Delta := \sqrt{9+8c^2} \qquad (7)$$

and

$$\theta := \frac{1}{3}\arctan\left(\frac{3\sqrt{3}\sqrt{54+117c^2+64c^4}}{27c+32c^3}\right) \qquad (8)$$

the minimum of v_x

$$x_{\min} = \frac{1}{3}d\left(\sqrt{2}\Delta\cos(\theta) + 2c\right) + x_0 \qquad (9)$$

and the two maxima are at

$$x_{\max\pm} = d\left(\frac{2}{3}c - \frac{\sqrt{2}}{6}\Delta\cos(\theta) \pm \frac{1}{\sqrt{6}}\Delta\sin(\theta)\right) + x_0\,. \qquad (10)$$

As we can verify easily, the quotient

$$\kappa(c) := \frac{x_+ - x_-}{x_{\min} - x_{\max-}} \qquad (11)$$

is a function of c only.

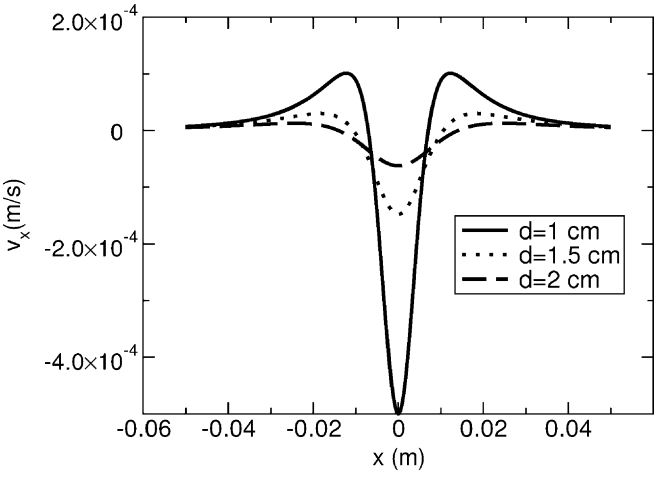

Fig. 6 As in Fig. 5, for $c = 0$ and different values of the distance d of the prey. The distance of the zeros is proportional to d

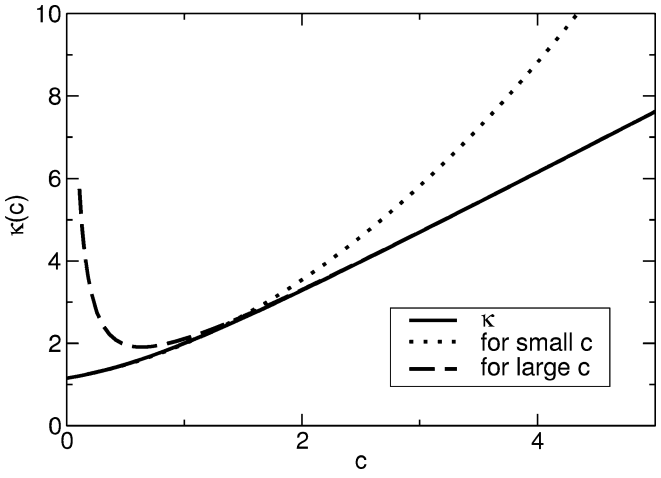

Fig. 7 The function $\kappa(c)$ and its Taylor approximation $\kappa(c) \approx \frac{2}{3}\sqrt{3} + \frac{\sqrt{2}}{3}c + \frac{5\sqrt{3}}{24}c^2$ at $c = 0$ as well as its asymptote $\kappa(c) = \frac{467}{768}\frac{1}{c} + \frac{3}{2}c$ for $c \to \infty$

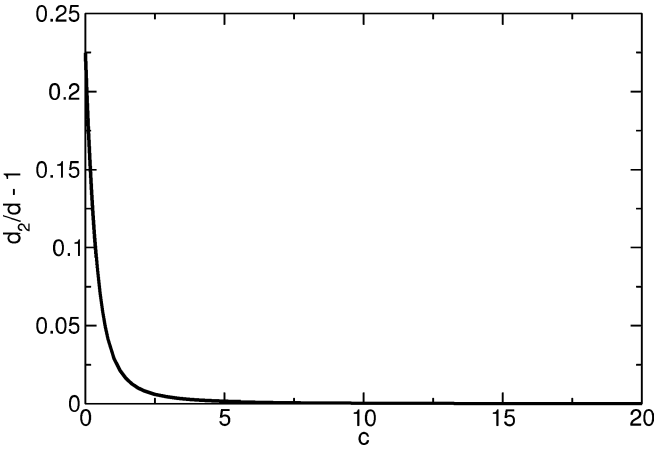

Fig. 8 Relative error $d_2/d - 1$ in the approximation of the distance d of (16) in dependency of c. The approximation is exact for $c \to \infty$

By measuring the zeros and the extrema of v_x, *Xenopus* can therefore determine c, as $\kappa(c)$ is a monotonic function of c, depicted in Fig. 7. E.g. neurons that react specifically to a maximum stimulus were found in the goldfish as well as in the mottled sculpin (Coombs et al. 1998). As soon as c is known the prey's distance d can be determined from the distance of the zeros in (6)

$$d = \frac{2(x_+ - x_-)}{\sqrt{9c^2 + 8}} \tag{12}$$

and the prey's position x_0 can be computed through

$$x_0 = \frac{x_+ + x_-}{2} - \frac{3}{4}cd\,. \tag{13}$$

We note that for "small" c, e.g. $c \leq 0.5$, which corresponds to an angle of $\alpha = 26^\circ$ between the velocity of the prey and the skin of the frog, the distance d as determined by (12) is approximately

$$d \approx d_1 := \frac{1}{\sqrt{2}}(x_+ - x_-)\,, \tag{14}$$

directly proportional to the distance between the zeros. Furthermore, because of (6)

$$x_0 \approx (x_+ + x_-)/2 \tag{15}$$

with a maximum error of $3d/8$. As the distance is underestimated for all values $c > 0$, the frog could continuously approach the prey, correct its orientation, and re-measure it until the prey is near enough.

As shown in Fig. 8, for large values of c we get

$$d \approx d_2 := x_{\min} - x_{\max -}\,. \tag{16}$$

If the distance d of the prey is too large or if the position x_0 is far away from the center of the animal, too few characteristic points (minimum, maxima and zeros) lie in the range of the lateral-line organs. Therefore, the animal can no longer determine the three unknowns c, d, and x_0 by considering characteristic points of v_x only. E.g., if $c = 0$ and $d >$ (length of the animal)$/\sqrt{2}$, the distance $x_+ - x_-$ between the zeros of v_x becomes larger than the length of the animal. In fact, experiments show that the longer a fish, the further away a given source can be detected (Denton and Gray 1989, Kalmijn 1989). On the other hand, if x_0 is "too" far away, the performance of the fish decreases (Coombs 1999).

3.2 Neuronal model

Xenopus has only inexact information about the velocities v_x because the velocities are encoded by the number of spikes that occur in the lateral-line nerves during a certain period of time, which must be assumed to be shorter than the response time of *Xenopus*, about 500–700 ms (Claas and Münz 1996). The neuronal model described below shows that the information *Xenopus* gets about the velocities v_x *suffices* to determine the distance d of the prey as well as its location x_0.

The firing rate of a lateral-line nerve in *Xenopus* depends logarithmically on the water velocity if the velocity is above a threshold of about $v_\vartheta := 0.05\,\mathrm{mm/s}$. The firing rate increases by about 40 Hz when the velocity doubles and saturates at 350 Hz for velocities beyond 10 mm/s. Below threshold, the (spontaneous) firing rate is about 50 Hz (Görner 1963), cf. also Strelioff and Honrubia (1978). We therefore model the firing rate $r(v)$ by

$$r(v) = \begin{cases} 50 & \text{for } v < v_\vartheta \\ 50 + 40\ln\left(\frac{v}{v_\vartheta}\right)/\ln(2) & \text{for } v \geq v_\vartheta \\ 350 & \text{for large } v \end{cases} \tag{17}$$

Each lateral-line organ is innervated by two nerves; the firing rate in one nerve increases for positive velocities v_x and vice versa. For a given v_x, the firing rate in a nerve sensitive for positive velocities is $r(v_x)$ so that the expectation value of the number of spikes that occur during a time T_R is $T_R\, r(v_x)$. In simulations T_R was set to be 500 ms. The number of spikes that occur in a nerve during an "experiment" is modeled as a Poissonian distribution with mean $T_R\, r(v_x)$. We denote by

$\#\{r(v_x)|T_R\}$ the number of spikes of a concrete realization of the process in a time interval of length T_R. To account for the information encoded in *both* nerves, one sensitive for positive velocities and the other one for negative velocities, in the neuronal model we estimate the velocity v_x at a certain lateral-line organ by

$$v_{\text{est}} = \gamma\,[\#\{r(v_x)|T_R\} - \#\{r(-v_x)|T_R\}] \tag{18}$$

so that v_{est} tends to be positive for $v_x > 0$ and negative otherwise. In the present context, γ is an irrelevant proportionality factor. We calculate velocities v_{est} for each lateral-line organ in an array of 50, with a distance of 1 mm between them. Then c is estimated by inverting $\kappa(c)$ in (11).

If $c < 1.5$, which corresponds to an angle of 56° between the velocity of the moving prey and the row of lateral-line organs, the model takes (12) to estimate the distance d and (13) to estimate the position x_0 of the prey. Else, the model takes (16) and $x_0 \approx (x_{\min} + x_{\max-})/2$. A neurophysiological hint that the neuronal system indeed uses the zeros of v_x is the fact that in the mottled sculpin there are neurons that react to a change in the sign of the pressure gradient (Coombs 1999). Simulations are shown in Figs. 9 and 10.

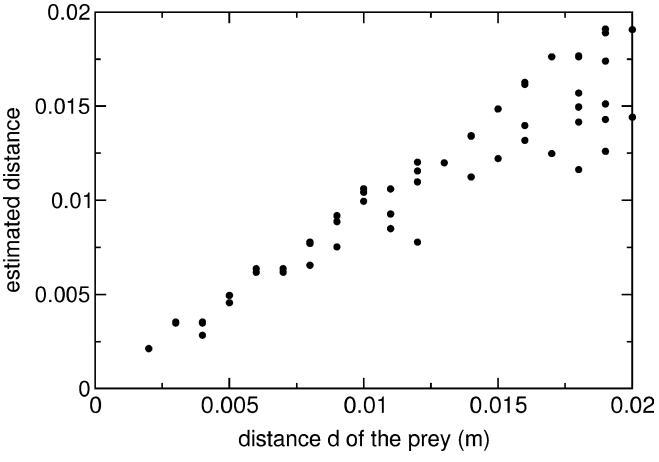

Fig. 9 The distance estimated by the neuronal model versus the true distance of the prey during 10 trials for each distance. The model parameters are $c = 0$, $w = 10$ cm/s, and $a = 1$ mm. At large distances (here about 2 cm) the model tends to undershoot the distance d whereas for small d it is quite accurate. Experiments with the mottled sculpin show the same trend (Coombs and Conley 1997)

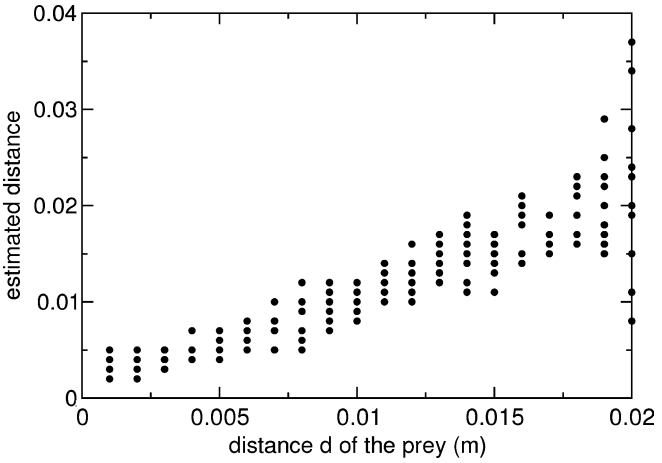

Fig. 10 As Fig. 9 but for $c = 100$. The velocity of the prey is now nearly perpendicular to the line of lateral-line organs. As is to be expected, the estimated distance scatters around the exact value

4 Model B: Optimal *Xenopus*

As yet there are no neuroanatomical data suggesting or supporting any model so that in addition to model A we now investigate a *minimal model* here, viz., answering the question of how *Xenopus* reconstructs the velocity of the moving object that has the highest probability under the influence of omnipresent noise. There are experimental data, however, clearly indicating the animal's ability to chase after small fish under water (van Netten 2005, personal communication). We suppose that in *Xenopus'* neuronal system, the velocity $\mathbf{w}$ of the moving object and its position $\mathbf{r}_0$ are determined by a maximum likelihood estimator. We thus have to maximize the likelihood or probability (van der Waerden 1969)

$$p(\mathbf{v}|\mathbf{w}, \mathbf{r}_0) \tag{19}$$

of the measured water velocities $\mathbf{v} = (v_1, \ldots, v_{180})$ at the lateral-line organs *given* the velocity $\mathbf{w}$ and the position $\mathbf{r}_0$ of the prey. As in model A, the only information that *Xenopus* has to determine the water velocities on its skin are action potentials coming from the nerves of the lateral-line system, resulting in inevitable errors.

Here we model these errors by adding a Gaussian random variable n_i with a standard deviation σ_n to the measured projections v_i of the water velocities onto *Xenopus'* skin. Although a Poissonian distribution of action potentials as taken in model A may be more appropriate, with Gaussian white noise the problem is mathematically tractable. We rewrite (3) as the exact velocity plus noise $v_i = \mathbf{t}_i(a, \mathbf{r}_i - \mathbf{r}_0) \cdot \mathbf{w} + n_i$. The likelihood in (19) is then

$$p(\mathbf{v}|\mathbf{w}, \mathbf{r}_0) = \frac{1}{\sqrt{2\pi\sigma_n^2}^{180}} \exp\left(-\frac{1}{2\sigma_n^2}\sum_{i=1}^{180} n_i(\mathbf{w}, \mathbf{r}_0)^2\right),$$

which can, according to the notation of (4), be written

$$p(\mathbf{v}|\mathbf{w}, \mathbf{r}_0) = \frac{1}{\sqrt{2\pi\sigma_n^2}^{180}} \exp\left\{-\frac{1}{2\sigma_n^2}[\mathbf{v} - T(a, \mathbf{r}_0)\mathbf{w}]^2\right\}. \tag{20}$$

Instead of maximizing the likelihood, we maximize its logarithm $\ln p(\mathbf{v}|\mathbf{w}, \mathbf{r}_0)$ so that we just have to maximize the expression

$$L(\mathbf{w}, \mathbf{r}_0) := -[\mathbf{v} - T(a, \mathbf{r}_0)\mathbf{w}]^2 \tag{21}$$

with respect to $\mathbf{w}$ and $\mathbf{r}_0$. Maximization with respect to $\mathbf{w}$ gives as a necessary condition

$$\frac{\partial L}{\partial \mathbf{w}}(\mathbf{w}, \mathbf{r}_0) = -\frac{2}{\sigma_n^2}\left(T^T\mathbf{v} - T^T T\mathbf{w}\right)\Big|_{\mathbf{w}=\hat{\mathbf{w}}} = 0$$

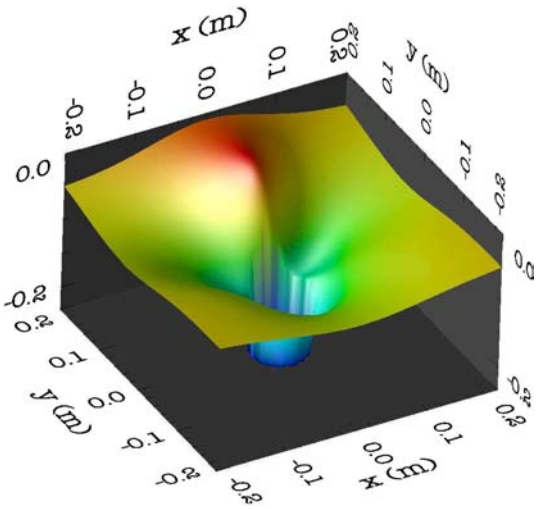

Fig. 11 The figure shows $L(\hat{\mathbf{w}}, \mathbf{r}_0)$ of model B's Eq. (21) at different positions $\mathbf{r}_0$ of a moving sphere. The sphere has a radius $a = 2\,\mathrm{cm}$ and moves at velocity $\mathbf{w} = (0, 1\,\mathrm{m/s}, 0)$ at position $(0, 0.1\,\mathrm{m}, 0)$. *Xenopus* is assumed to have 180 lateral-line organs arranged, for the sake of computational convenience, in two circles in the x, y-plane, where 90 organs are most sensitive for velocities tangential to the boundary of the circle and 90 organs are most sensitive for velocities in z-direction. For simplicity, there was no noise, i.e., $\sigma_n = 0$. At the position $(0, 10\,\mathrm{cm}, 0)$, where the sphere is located, L has a maximum. That is, the position of the sphere can be determined

for the maximum $\hat{w}$, which leads to the linear system of equations

$$\left(T^T T\right) \hat{\mathbf{w}} = T^T \mathbf{v}\,.$$

If we denote the pseudo-inverse (Press et al. 1995) of the matrix $T^T T$ by $\left(T^T T\right)^\dagger$, the solution with minimal $\|\mathbf{w}\|$ is $\hat{\mathbf{w}} = \left(T^T T\right)^\dagger T^T \mathbf{v}$ where $T = T(a, \mathbf{r}_0)$. Figure 11 shows numerical results for $L(\hat{\mathbf{w}}, \mathbf{r}_0)$ at different positions $\mathbf{r}_0$ of a moving sphere. Figure 12 shows that it is not only possible to reconstruct the position but also the velocity of the moving sphere.

To test whether it is still possible for *Xenopus*, using the method suggested here, to determine the position of a submerged moving sphere under noisy conditions, noise was applied to the simulation shown in Fig. 13. A standard deviation of the noise of $\sigma_n = 10^{-4}\,\mathrm{m/s}$ seems plausible because this is the velocity threshold for *Xenopus'* lateral line organs (Bleckmann 1994). Clearly, *Xenopus* could still determine the position of a moving sphere under noisy conditions. Figure 14 shows that it is indeed possible to determine the distance under noisy conditions independently of the velocity of the moving sphere.

5 Discussion

It is as yet unknown how precisely under-water detection of moving objects by fish and other animals works, performed solely by analyzing the local water velocities caused by the moving object. The model presented here demonstrates how

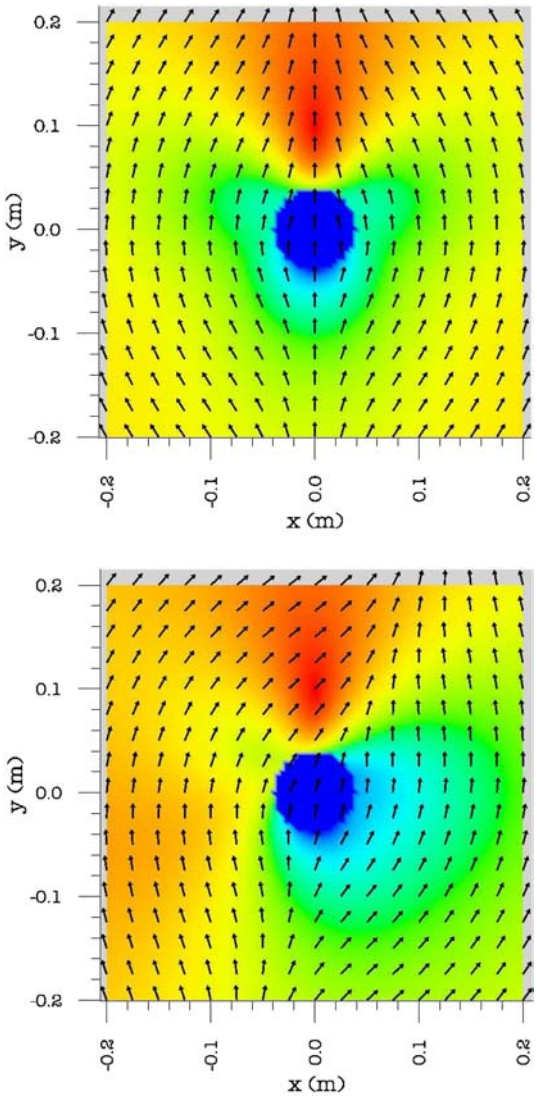

Fig. 12 The upper panel shows $L(\hat{\mathbf{w}}, \mathbf{r}_0)$ (color-coded) of model B with the same parameters as in Fig. 11. The arrows additionally indicate the directions $\hat{\mathbf{w}}/|\hat{\mathbf{w}}|$ of the reconstructed velocities of the moving sphere at different assumed positions $\mathbf{r}_0$ of the sphere. At the true position $(0, 10\,\mathrm{cm}, 0)$, the reconstructed direction of the velocity $\hat{\mathbf{w}} = (0, 1\,\mathrm{m/s}, 0)$ is accurate. In the lower panel, the velocity of the moving sphere is $\hat{\mathbf{w}} = (1, 1, 0)$, which is also reconstructed appropriately

Xenopus could *in principle* accomplish localization of a moving object by using the inputs from the lateral-line organs only. Both models are able to localize moving objects. Model A is a neuronal model that performs short-range localization only from characteristic points (minimum, maxima and zeros) of the measured water velocities v_x and is thus robust against almost any monotonic nonlinear distortion of v_x by nonlinear neuronal transducers. Model B can even localize the object in full three dimensions, as well as determine its velocity and 3d-direction of motion. Model B also accounts for the fact that *Xenopus* uses 180 lateral-line organs that are distributed around its body and have different orientation. In contrast, for model A a linear arrangement of lateral-line organs with a single orientation is sufficient, as found in many

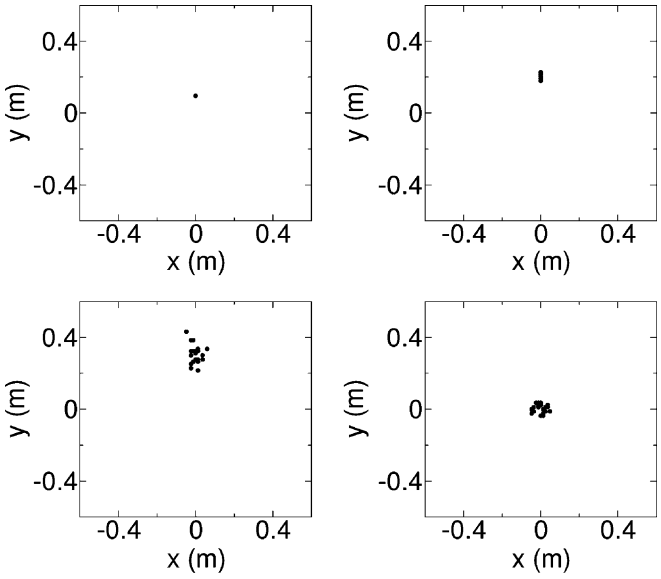

Fig. 13 The dots show the positions $\mathbf{r}_0$ where $L(\hat{\mathbf{w}}, \mathbf{r}_0)$ had a maximum in 25 different runs. The position of the moving sphere with velocity $\mathbf{w} = (0, 1\,\mathrm{m/s}, 0)$ was at 10, 20, 30 cm and at infinite distance in y-direction from left to right and top to bottom. The standard deviation of the noise is $\sigma_n = 10^{-4}$ and all other parameters are the same as in Fig. 11. Although noise is present, the position of the sphere can be determined rather accurately up to about 30 cm

fish. The models developed here for superficial neuromasts, i.e. velocity detectors, can in principle also be applied to many fish, e.g. goldfish, that use their superficial neuromasts to detect prey in still water (Vogel and Bleckmann 2001).

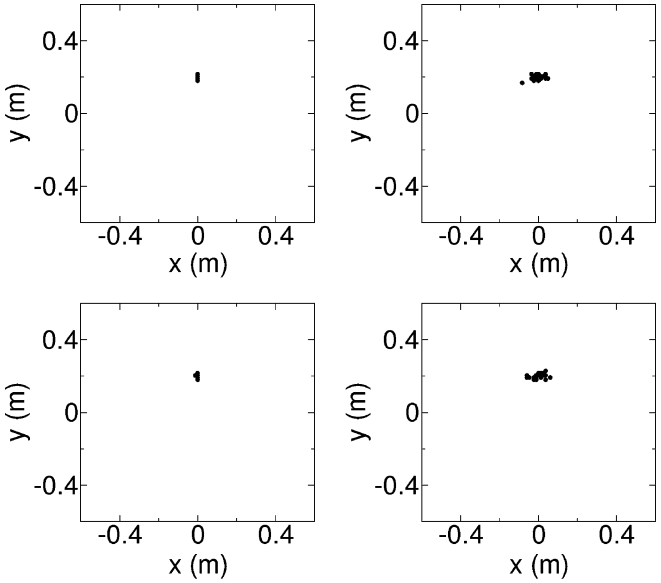

Fig. 14 Same type of plot as in Fig. 13. The y-coordinate of the moving sphere is fixed at $y = 20$ cm while its velocity is $\mathbf{w} = (0, 1\,\mathrm{m/s}, 0)$, $(1\,\mathrm{m/s}, 0, 0)$, $(0, -1\,\mathrm{m/s}, 0)$, and $(-1\,\mathrm{m/s}, 0, 0)$ from left to right and top to bottom. *Xenopus* being at the origin, its performance is best when the prey's position **r** and velocity **w** are parallel and worst when **r** and **w** are perpendicular

References

Bleckmann H (1994) Reception of Hydrodynamic Stimuli in Aquatic and Semiaquatic Animals. Fischer, Stuttgart

Braess D (2003) Finite Elemente. 3. Aufl. Springer, Berlin

Claas B, Münz H (1996) Analysis of surface wave direction by the lateral line system of Xenopus: Source localization before and after inactivation of different parts of the lateral line. J Comp Physiol 178(2):253–268

Coombs S (1999) Signal detection theory, lateral-line excitation patterns and prey capture behaviour of mottled sculpin. Animal Behavior 58:421–430

Coombs S, Conley RA (1997) Dipole source localization by mottled sculpin: I. Approach strategies. J Comp Physiol 180(4):387–399.

Coombs S, Fay RR (1993) Source level discrimination by the lateral line system of the mottled sculpin, Cottus bairdi. J Acoust Soc Am 93(4):2116–2123

Coombs S, Finneran JJ, Conley RA (2000) Hydrodynamic image formation by the peripheral lateral line system of the Lake Michigan mottled sculpin, Cottus bairdi. Phil Trans R Soc Lond B 355(1401):1111–1114

Coombs S, Mogdans J, Halstead M, Montgomery J (1998) Transformation of peripheral inputs by the first-order lateral line brainstem nucleus. J Comp Physiol A 182:609–626

Denton EJ, Gray JAB (1989) Some observations on the forces acting on neuromasts in fish lateral line canals. In: Coombs S, Görner P, Münz H (eds) The Mechanosensory Lateral Line: Neurobiology and Evolution. Springer, New York, pp 229–246

Elepfandt A (1984) The role of ventral lateral line organs in water wave localization in the clawed toad (*Xenopus laevis*). J Comp Physiol A 154:773–780

Elepfandt A. (1996). Sensory perception and the lateral line system in the clawed frog, *Xenopus*. In: Tinsley RC, Kobel HR, (eds) The Biology of Xenopus. chap. 7, p 97–120. Clarendon Press, Oxford

Engelmann J, Kröther S, Bleckmann H, Mogdans J (2003) Effects of running water on lateral line responses to moving objects. Brain Behav Evol 61:195–212

Franosch JMP, Lingenheil M, van Hemmen JL (2005) How a frog can learn what is where in the dark. Phys Rev Lett 95:078106–1/4

Franosch JMP, Sobotka MC, Elepfandt A, van Hemmen JL (2003) Minimal model of prey localization through the lateral-line system. Phys Rev Lett 91:158101–1/4

Griebel M, Dornseifer T, Neunhoeffer T (1995) Numerische Simulation in der Strömungsmechanik: eine praxisorientierte Einführung. Vieweg, Braunschweig

Görner P (1963) Untersuchungen zur Morphologie und Elektrophysiologie des Seitenlinienorgans vom Krallenfrosch (*Xenopus laevis* Daudin). Z vergl Physiol 47:316–338

Görner P, Mohr C (1989) Stimulus localization in *Xenopus*: Role of directional sensitivity of lateral line stitches. In: Coombs S, Görner P, Münz H (eds) The Mechanosensory Lateral Line: Neurobiology and Evolution. Springer, New York, pp 543–560

Hackbusch W (1986) Theorie und Numerik elliptischer Differentialgleichungen. Teubner

Hassan ES (1985) Mathematical analysis of the stimulus for the lateral line organ. Biol Cybern 52(1):23–36

Hofmann MH, Falk M, Wilkens LA (2004) Electrosensory brain stem neurons compute the time derivative of electric fields in the paddlefish. Fluct Noise Lett 4:L129–L138

Kalmijn AJ (1988) Hydrodynamic and acoustic field detection. In: Atema J, Fay RR, Popper AN, Tavolga WN (eds) Sensory Biology of Aquatic Animals. Springer, New York, pp 83–130

Kalmijn AJ (1989) Functional evolution of lateral line and inner ear sensory systems. In: Coombs S, Görner P, Münz H (eds) The Mechanosensory Lateral Line: Neurobiology and Evolution. Springer, New York, pp 187–215

Kramer G (1933) Untersuchungen über die Sinnesleistungen und das Orientierungsverhalten von Xenopus laevis Daud. Zool Jb Physiol 52:629–676

Lamb H (1932) Hydrodynamics. Cambridge University Press, Cambridge, 6th edn. §§226ff, 246, 331, 332

Marsal D (1989) Finite Differenzen und Elemente - Numerische Lösung von Variatonsproblemen und partielle Differentialgleichungen. Springer, Berlin

Press WH, Teukolsky SA, Vetterling WT, Flannery BP (1995) Numerical Recipes in C. Cambridge University Press

Roache PJ (1972) Computational fluid dynamics. Hermosa Publishers, Albuquerque

Russell IJ (1976) Amphibian lateral line receptors. In: Llinas R, Precht W, (eds) Frog Neurobiology: A Handbook. 513–550. Springer, Berlin

Strelioff D, Honrubia V (1978) Neural transduction in *Xenopus laevis* lateral line system. J Neurophysiol 41(2):432–444

Tinsley RC, Kobel HR (Eds.) (1996) The Biology of Xenopus. Clarendon Press, Oxford

van der Waerden BL (1969) Mathematical Statistics. Springer, Berlin

Varga RS (1999) Matrix Iterative Analysis. Springer Series in Computational Mathematics. Springer, 2nd edn

Vogel D, Bleckmann H (2001) Behavioral discrimination of water motions caused by moving objects. J Comp Physiol A 186:1107–1117

Young DM (1971) Iterative Solution of Large Linear Systems - Computer Science and Applied Mathematics. Academic Press, New York